

Microscopic model, spin wave theory, and competing orders in double perovskites

G. Jackeli*

Institut Laue Langevin, B. P. 156, F-38042, Grenoble, France

We present a microscopic theory of carrier-induced ferrimagnetism in metallic double perovskite compounds such as $\text{Sr}_2\text{FeMoO}_6$ and $\text{Sr}_2\text{FeReO}_6$ which have recently attracted intense interest for their possible applications to magnetotransport devices. We find half-metallic ferrimagnetic state for carrier density n below a critical value n_{cr} and predict layered antiferromagnetic structure for $n > n_{cr}$. We study spin wave spectrum including quantum corrections and find strongly enhanced quantum effects in the vicinity of zero-temperature phase transition.

PACS numbers:75.10.Lp, 75.30.Ds, 75.30.Vn

The recent discovery of the room temperature magnetoresistance in double perovskite (DP) compounds [1] has generated intense interest in these materials because of their potential importance as magnetotransport devices as well as their rich and challenging physical properties. For applications metallic ferrimagnetic compounds such as $\text{Sr}_2\text{FeMoO}_6$ and $\text{Sr}_2\text{FeReO}_6$ are of particular interest, because both have high magnetic transition temperature ($T_c \simeq 420$, and $\simeq 400$ K, respectively) and their electronic structures have been suggested to be half-metallic [1].

Despite an enormous interest in half-metallic ferromagnets, most of the theoretical studies until now have been only by *ab initio* methods [2–5]. The obtained results differ qualitatively and the cause of ferrimagnetism is still controversial (see, for example, [4]). Moreover, band theories are based on a single-particle picture, an approximation that is questionable when local moments of Fe are formed, i.e. when strong local correlations suppress electron density fluctuations in a half-filled $3d$ -shell. More detailed theoretical study based on an alternative approach is thus highly desirable.

In this letter we formulate a new microscopic theory of the carrier-induced ferrimagnetism in this family of magnetic compounds. The theory is based on a minimal model Hamiltonian, in which only the lowest energy charge fluctuations, coupled to the local moments, are retained, and those which are moved to high energies due to strong correlations, are disallowed. The model has two parameters and allows for reliable analytical treatment of the physically relevant situation.

In the DP structure Fe and Mo/Re ions form two face centered cubic sublattices and each pair of nearest-neighbor lattice sites is occupied by two different ions. In the ionic picture, Fe is in the $3+$ valence state and half-filled d -shell forms a $S = 5/2$ local moment. The Mo is in $5+$ valence state with one t_{2g} electron in $4d$ -shell (see, for example, [2]). This extra electron, which hybridizes with the same orbital states at the neighboring iron sites, is responsible for the system's lowest energy charge excitations [6]. In the classical picture, only a spin down electron, with respect to a neighboring Fe

local moment, can hop to this Fe site. For a spin up electron this hopping is blocked by the Pauli principle, as at the iron site the spin up states are already all occupied. Thus, *it is the exclusion principle*, which couples the itinerant spins and the local moments *kinematically*. This contrasts with the case of double-exchange systems, in which the intra-atomic Hund's rule is responsible for the coupling between the two subsystems [7]. In the magnetic double perovskites, as in double exchange magnets, ordering of local moments occurs due to the reduction of the kinetic energy. The kinetic energy in DPs compounds is minimized when the local moments are parallel to each other and antiparallel to itinerant spins, and this causes the ferrimagnetism.

Model Hamiltonian. — We now turn to a minimal model Hamiltonian reflecting the above discussion. We retain only low energy charge excitations in the system, which correspond to the processes $(\text{Fe } d^5, \text{B}' d^n) \leftrightarrow (\text{B } d^6, \text{Fe}' d^{n-1})$ (B' stands for Mo/Re). The Fe ions are treated as localized spins $S = 5/2$ and extra electrons from nonmagnetic Mo/Re ions as charge carriers. There are $n = 1$ and $n = 2$ carriers per unit cell in Mo and Re compounds, respectively. When a carrier is placed at a site with core spin $S = 5/2$, the total spin \mathcal{S} can take two possible values $\mathcal{S} = 2$ and $\mathcal{S} = 3$. However, the maximal allowed spin for six electrons in a d -shell is $\mathcal{S} = 2$. To project out the $\mathcal{S} = 3$ spin state we introduce infinite local antiferromagnetic (AFM) coupling $J \rightarrow \infty$ between core and itinerant spins [8]. The carriers occupy three degenerate t_{2g} (d_{xy}, d_{yz}, d_{yz}) orbital states. In the cubic lattice the t_{2g} -transfer matrix is diagonal in the orbital space and is non-zero only in the corresponding plane. A minimal Hamiltonian can be written as a sum of three two dimensional (2D) terms $\mathcal{H} = H_{xy} + H_{xz} + H_{yz}$, where each term corresponds to a given orbital state. All three terms have the same form given by (we further omit orbital index for simplicity)

$$H = -t \sum_{ij\sigma} d_{i\sigma}^\dagger d_{j\sigma} + \sum_{i(j)} \{ \Delta [n_i - n_j] + J [\mathbf{S}_i \mathbf{s}_i - A n_i] \}, \quad (1)$$

where $i(j)$ labels Fe (Mo/Re) ions, t is an electron trans-

fer integral between nearest-neighbor Fe and (Mo/Re) ions, $\Delta = E(\text{Fed}^6, B'd^0) - E(\text{Fed}^5, B'd^1)$ is a charge transfer gap, and \mathbf{S}_i (s_i) stands for the localized (itinerant) spin. The last constant term, where $A = (S + 1)/2$, is chosen so that the exchange energy vanishes for a state with $S = 2$.

We now consider the ferromagnetic (FM) arrangement of local moments, which corresponds to the ground state of Hamiltonian (1) for carrier density $n < n_{cr}$ (see below). In the limit $J \rightarrow \infty$, we restrict the Hilbert space to spin eigenstates with maximum allowed spin S at a given site. Thus, the magnetic ion is in a state either with $S = S$, without an extra electron, or of $S = S - 1/2$, with an extra electron. The site states are labeled by $|\mathcal{S}, M\rangle$ and M is z -projection of the spin \mathcal{S} . Considering low lying excitations we can retain only the states with $M = S$ and $M = S - 1$. Then the local Hilbert space consists of four states: $|\mathcal{S}, S\rangle$, $|\mathcal{S}, S - 1\rangle$, $|S - \frac{1}{2}, S - \frac{1}{2}\rangle$, and $|S - \frac{1}{2}, S - \frac{3}{2}\rangle$. To describe transitions between these states we introduce magnon and fermion operators as $B^\dagger|\mathcal{S}, M\rangle = |\mathcal{S}, M - 1\rangle$ and $D_\downarrow^\dagger|\mathcal{S}, M\rangle = |S - \frac{1}{2}, M - \frac{1}{2}\rangle$, respectively. Through corresponding matrix elements, one can find the following relations $d_\downarrow = D_\downarrow [1 - B^\dagger B/4S - B^\dagger B/(32S^2)]$, and $d_\uparrow = -D_\downarrow B^\dagger/\sqrt{2S}$ to order $1/S^2$. The state generated by D_\uparrow corresponds to $S = S + 1/2$ and is projected out.

As a next step, we express the Hamiltonian (1) in terms of the new operators, diagonalize its band part, and arrive in the momentum space to the following expression $H = H_0 + H_1 + H_2$, where

$$\begin{aligned}
H_0 &= \sum_{\mathbf{k}} \left\{ E_{\mathbf{k}} [a_{\mathbf{k}\downarrow}^\dagger a_{\mathbf{k}\downarrow} - b_{\mathbf{k}\downarrow}^\dagger b_{\mathbf{k}\downarrow}] - \Delta d_{\mathbf{k}\uparrow}^\dagger d_{\mathbf{k}\uparrow} \right\}, \\
H_1 &= \frac{1}{\sqrt{2SN}} \sum_{\mathbf{k}, \mathbf{q}} \left\{ d_{\mathbf{k}-\mathbf{q}\uparrow}^\dagger [N_{\mathbf{k}, \mathbf{q}} a_{\mathbf{k}\downarrow} + M_{\mathbf{k}, \mathbf{q}} b_{\mathbf{k}\downarrow}] B_{\mathbf{q}}^\dagger + \text{H.c.} \right\}, \\
H_2 &= \frac{1}{4SN} \left[1 + \frac{1}{8S} \right] \sum_{\mathbf{k}, \mathbf{p}, \mathbf{q}} B_{\mathbf{q}}^\dagger B_{\mathbf{q}+\mathbf{p}-\mathbf{k}} \left\{ P_{\mathbf{k}, \mathbf{p}}^{aa} a_{\mathbf{k}\downarrow}^\dagger a_{\mathbf{p}\downarrow} \right. \\
&\quad \left. + P_{\mathbf{k}, \mathbf{p}}^{bb} b_{\mathbf{k}\downarrow}^\dagger b_{\mathbf{p}\downarrow} + P_{\mathbf{k}, \mathbf{p}}^{ab} [a_{\mathbf{k}\downarrow}^\dagger b_{\mathbf{p}\downarrow} + \text{H.c.}] \right\}. \quad (2)
\end{aligned}$$

The first term H_0 , corresponding to the classical limit ($S \rightarrow \infty$), describes the band structure of the system. The electronic structure of each orbital state is composed of the three bands: bonding and antibonding of down spin, and nonbonding of up spin electrons. $E_{\mathbf{k}} = \sqrt{\varepsilon_{\mathbf{k}}^2 + \Delta^2}$ and $\varepsilon_{\mathbf{k}} = 2t(\cos k_x + \cos k_y)$ for the d_{xy} -orbital. For n carriers per unit cell each bonding band of a given orbital is $n/3$ -filled and fully polarized. Given this band structure, the system is half-metallic for arbitrary model parameters (t, Δ) and for any realistic value of carrier density.

The last two terms H_1 and H_2 [see Eq.(2)] are due to the quantum nature of the core spins. Spin up electrons, localized in the classical picture, can move thanks to the quantum nature of the local moments, but leaving

a trace of spin deviations along their trajectories. This process is described by H_1 . The last term H_2 describes fluctuations of the local moment generated by the hopping of spin down electrons. The corresponding vertices are given by $N_{\mathbf{k}, \mathbf{q}} = \varepsilon_{\mathbf{k}-\mathbf{q}} u_{\mathbf{k}}$, $M_{\mathbf{k}, \mathbf{q}} = \varepsilon_{\mathbf{k}-\mathbf{q}} v_{\mathbf{k}}$, $P_{\mathbf{k}, \mathbf{p}}^{aa} = -\varepsilon_{\mathbf{k}} v_{\mathbf{k}} u_{\mathbf{p}} - \varepsilon_{\mathbf{p}} u_{\mathbf{k}} v_{\mathbf{p}}$, $P_{\mathbf{k}, \mathbf{p}}^{bb} = \varepsilon_{\mathbf{k}} u_{\mathbf{k}} v_{\mathbf{p}} + \varepsilon_{\mathbf{p}} v_{\mathbf{k}} u_{\mathbf{p}}$, and $P_{\mathbf{k}, \mathbf{p}}^{ab} = \varepsilon_{\mathbf{p}} u_{\mathbf{p}} u_{\mathbf{k}} - \varepsilon_{\mathbf{k}} v_{\mathbf{k}} v_{\mathbf{p}}$, where $u(v)_{\mathbf{k}} = \sqrt{[1 \pm \Delta/E_{\mathbf{k}}]/2}$.

Spin wave theory. – We now turn to analysis of the spin wave spectrum. As the value of the core spin is relatively large $S = 5/2$ we perform the $1/S$ expansion of a spin wave self-energy. The magnon Green function is obtained from the Dyson equation $D_{\mathbf{q}, \omega} = [\omega - \Sigma_{\mathbf{q}, \omega}]^{-1}$. To order $1/S$, the self-energy Σ includes the second order perturbative contribution from H_1 as well as first order contribution from H_2 (see first two diagrams in Fig. 1.) (The analytical form of Σ is lengthy and will be presented elsewhere.) Here we discuss the results. There are two branches of spin excitations, like those of localized ferromagnets, the gapless Goldstone mode and the optical mode. In addition to this, there exists a Stoner continuum of spin-flip particle-hole excitations.

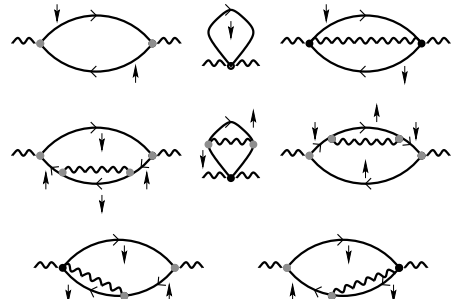


FIG. 1. The leading order ($1/S$) and next-to-leading order ($1/S^2$) spin wave self-energies. Wave (solid) line stands for the magnon (electron) propagator. The small arrow denotes an electron spin and gray (black) dot stands for the magnon-electron vertex proportional to $1/\sqrt{S}$ ($1/S$).

We below focus on the low energy mode. The spectrum of the magnons at the quasi-classical level is Heisenberg-like $\omega_{\mathbf{q}} = 16SJ_1[1 - \gamma_{1\mathbf{q}}] + 16SJ_2[1 - \gamma_{2\mathbf{q}}]$, where J_1 and J_2 are nearest and next-nearest neighbor exchange couplings, respectively, $\gamma_{1\mathbf{q}} = (\cos q_x \cos q_y + \cos q_x \cos q_z + \cos q_y \cos q_z)/3$, and $\gamma_{2\mathbf{q}} = (\cos^2 q_x + \cos^2 q_y + \cos^2 q_z)/3$. The carrier-induced exchange energies are given by $J_{1(2)} = t^2/(16S^2N) \sum_{\mathbf{k}} \bar{\gamma}_{1(2)} n_{\mathbf{k}}/E_{\mathbf{k}}$, where $\bar{\gamma}_1 = 2 \cos k_x \cos k_y$, $\bar{\gamma}_2 = \cos 2k_x + \cos 2k_y$ and $n_{\mathbf{k}}$ is a Fermi distribution function. We also note that there is no Landau damping of spin waves at this order.

In Fig. 2(a) we show carrier density dependence of the spin stiffness $\mathcal{D} = 16S(J_1 + J_2)$ for different values of Δ . At a fixed density the stiffness scales with the bandwidth: $\mathcal{D} \sim t$ for $t \gg \Delta$ and $\mathcal{D} \sim t^2/\Delta$ for $t \ll \Delta$. As a function of density the spin stiffness exhibits strongly nonmonotonic behavior. It shows a maximum at optimal filling $n_{opt} \simeq 1$ and then drops to zero at some critical

density n_{cr} [9].

We now analyze quantum corrections to the harmonic spectrum discussed above. These corrections are generated by the magnon self-energy diagrams proportional to $1/S^2$ [10]. They are governed by fermionic excitations and are thus different from those in insulating magnets. At this order magnon self-energy includes fourth and second order contributions from H_1 and H_2 , respectively, as well as mixed type terms. Graphically they are presented in Fig. 1. From the structure of the diagrams one easily verifies that renormalization of the electron propagator due to the scattering of spin waves as well as all relevant vertex corrections are consistently taken into account at this order. After collecting all the diagrams in this order one recovers the Goldstone theorem, that guarantees the consistency of the approximation.

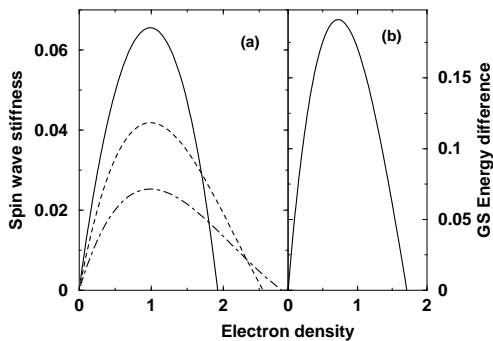


FIG. 2. (a) Spin wave stiffness (in units of $t = 1$) versus carrier density, for different values of Δ ($\Delta = 0, 4$, and 8 , solid, dashed and dotted-dashed lines, respectively); (b) Ground state (GS) energy difference (in units of t , and for $\Delta = 0$) between AFM-II and ferrimagnetic states versus carrier density.

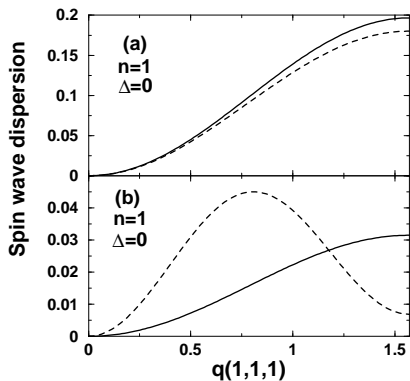


FIG. 3. Spin wave spectrum in [111] direction (in units of $t = 1$) versus momentum. Solid and dashed lines represent the harmonic and renormalized magnon dispersion law, respectively.

The quantum corrections generate two main effects in the magnon spectrum: (i) they give rise to spin wave damping in the ground state, and (ii) they modify the semi-classical dispersion law of magnons. The

first nonzero contribution to magnon damping $\Gamma_{\mathbf{q}}$ is proportional to $1/S^3$ and is due to the spin wave scattering of carrier density fluctuations. To evaluate damping, one has to replace the bare magnon propagator in the self-energy diagrams by that obtained in harmonic approximation (see Golosov in Ref. [10]). In the long wave-length limit one finds $\Gamma_{\mathbf{q}} \propto \langle f_{k_F} \rangle t q^6 / S^3$, where $\langle f_{k_F} \rangle$ denotes the Fermi surface average of $f_{\mathbf{k}} = (\sin k_x + \sin k_y)^2$.

Figure 3 shows magnon dispersion obtained semiclassically (solid line) and with quantum corrections included (dashed line), for carrier densities $n = 1$, Fig.3(a), and $n = 1.8$, Fig.3(b). In the case of optimal carrier density, $n = 1$, the quantum effects are small and practically do not alter harmonic dispersion law. However, for a higher carrier density the quantum effects become strongly pronounced and result in a dramatic modification of the harmonic spectrum. They cause stiffening of the long-wave length excitations and strong softening of the zone boundary magnons [see Fig. 3(b)].

Instability of ferrimagnetic ordering. – As we have already mentioned, there is a critical carrier density n_{cr} at which the spin wave stiffness vanishes [see Fig. 2(a)]. This indicates that there exist another type of magnetic ordering which competes with ferrimagnetic order and becomes favorable as $n \rightarrow n_{cr}$. The most direct route to identify the symmetry of new magnetic order is to find the wave vector at which spin wave spectrum becomes unstable. The linear theory can not answer this question, because the harmonic dispersion vanishes identically in [111] direction, and no special soft mode is singled out at this order. The problem can be resolved by considering quantum effects. The tendency of the zone boundary magnons to soften with increasing n [see Fig. 2(a) and 2(b)] can be interpreted as a precursor effect of a transition to a layered magnetic ordering with wave-vector $\mathbf{Q} = \pi/2[1, 1, 1]$. The latter consists of alternating {111} FM planes. The magnetic moments of neighboring planes can be either misaligned by an angle θ , which is the case of canted magnetic structure, or aligned antiparallel to form type-II antiferromagnetic (AFM-II) ordering. Hence, there are two possible scenarios for the phase transition: (a) the transition is second order and is to a canted state or (b) transition is first order directly to AFM-II ordering. To decide which of these two is realized we have evaluated and compared the kinetic energy of carriers in ferrimagnetic, canted and AFM-II background of core spins. We have found that canted state never minimizes the energy and hence is never stabilized.

In Fig. 4 (left panel) we show 2D (001) cut of AFM-II magnetic structure. In this magnetic structure carriers are confined within the 1D FM stripes and have the dispersion law $\varepsilon_k = -2\sqrt{2}t \cos k$ (the factor $\sqrt{2}$ is due to the two possible path of the charge transfer between nearest-neighbor magnetic ions). Figure 2(b) shows the difference between the energies (ΔE) of the AFM-II and ferrimagnetic states versus carrier density. As it is seen

in this figure, with increasing carrier density ΔE shows the same trend, not coincidentally, as the spin wave stiffness [see Fig. 2(a)], and also vanishes at $n \simeq n_{cr}$. For $n > n_{cr}$ carriers gain more kinetic energy in AFM-II state. Based on the above analysis, in Fig. 4 (right panel) we propose a schematic phase diagram of Hamiltonian (1). The dashed curve, in this figure, denote the second order phase boundary between paramagnetic and magnetically ordered states. The ferrimagnetic phase is stable for carrier density $n < n_{cr}$ and there is a first order phase transition to AFM-II ordering at $n = n_{cr}$. The first order phase boundary [see solid line in Fig.4] is terminated by the bicritical point.

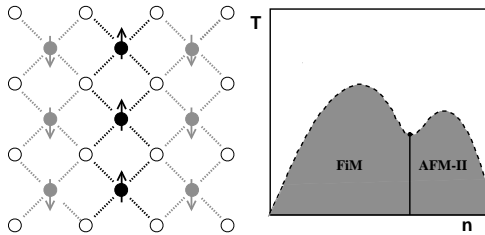


FIG. 4. Left panel: Two dimensional (001) cut of the AFM-II structure. Filled (opened) circles denote Fe (Mo/Re) ions and big arrows stand for the core spins. Black (grey) dashed lines indicate the allowed path for spin down (up) electrons; Right panel: schematic phase diagram of model (1) in (T, n) plane.

So far, we have not considered the effect of direct AFM exchange J' between the local moments. At the semi-classical level, an effect of J' is to reduce carrier-induced FM exchange. However, in the compounds with large transfer gap Δ , FM exchange can be largely suppressed and AFM exchange, if strong enough, can stabilize AFM-II magnetic ordering. Considering the metallic compounds with fully polarized carriers we have also neglected interaction between charge carriers. The carrier correlation effects become relevant for large Δ , when carriers are mostly confined in one sublattice, and/or for a higher carrier density. In the both situations, the ground state shows AFM-II ordering. In AFM-II background the carrier band is nearly one dimensional. In this case both correlations and any disorder renders 1D system insulating. Indeed, the insulating antiferromagnetic state has been observed in Sr_2FeWO_6 compound.

Summary. – To summarize we have presented a microscopic theory of metallic magnetic double-perovskites. We conclude that these compounds form a new class of magnetic materials whose properties are entirely determined by the presence of magnetic (B=Fe) as well as nonmagnetic (B'=Fe/Re) transition metal ions in their structures. Our approach allows for a reliable description of the physically relevant situation in which charge carriers are constrained to be antiparallel to Fe local moments. Our findings are as follows.

We find ferrimagnetic ground state for carrier density

$n < n_{cr}$ and predict the type-II layered antiferromagnetic structure for $n > n_{cr}$. In the ferrimagnetic state charge carriers are fully polarized and their electronic structure is half-metallic. An effective local exchange splitting on B sites is infinite and is zero on nonmagnetic B' sites. The spin degeneracy on B' sites is lifted kinematically. The half-metallicity is a robust feature of ferrimagnetic ground state for arbitrary values of model parameters. Zero-temperature spin stiffness exhibits a strongly non-monotonic variation with the carrier density. The highest value of spin stiffness is realized when the energy level of Fe d^6 configuration is at resonance with B' d -level and there is one charge carrier per unit cell [9]. At the semiclassical level, spin excitations above the ferrimagnetic ground state have a Heisenberg-like dispersion law. However, quantum effects become strongly pronounced in the vicinity of zero-temperature phase transition, as $n \rightarrow n_{cr}$, and cause strong modification of harmonic dispersion law. We suggest that Re compounds, which have higher band filling, are more likely to exhibit interesting quantum effects in spin dynamics. This may be directly detected by inelastic neutron scattering experiments.

We thank N. Andrei, E. I. Kats, D. I. Khomskii, D.E. Logan, and Ph. Nozières for their interests and useful discussions. Earlier discussion with D. D. Sarma is gratefully acknowledged. We are indebted to M. E. Zhitomirsky for continuous valuable discussions and to T. Ziman for a critical reading of the manuscript.

* On leave from E. Andronikashvili Institute of Physics, Georgian Academy of Sciences, Tbilisi, Georgia.

- [1] K.-I. Kobayashi *et al.*, Nature (London) **395**, 677 (1998); K.-I. Kobayashi *et al.*, Phys. Rev. B **59**, 11159 (1999).
- [2] D. D. Sarma *et al.*, Phys. Rev. Lett. **85**, 2549 (2000); S. Ray *et al.*, *ibid.* **87**, 097204 (2001).
- [3] Z. Fang, K. Terakura, and J. Kanamori, Phys. Rev. B **63**, 180407 (2001).
- [4] I. V. Solovyev, Phys. Rev. B **65**, 144446 (2002).
- [5] T. Saitoh *et al.*, Phys. Rev. B **66**, 035112 (2002).
- [6] This is supported by the observation that there is no evidences of presence of $\text{Fe}^{+1}(d^4)$ in the ground state.
- [7] Since completing this work we have become aware of work, D. D. Sarma, Cur. Opin. Solid State Mat. Sci. **5**, 261 (2001), in which a similar point was made.
- [8] We have recently learned that limit $J \rightarrow \infty$ has been also discussed by E. L. Nagaev (cond-mat/0204308), however in a different context. We thank D. I. Khomskii for pointing this to us.
- [9] This is in agreement with the dynamical mean-field study of a somewhat extended Hamiltonian by A. Chattopadhyay and A. J. Millis, Phys. Rev. B **64**, 024424 (2001).
- [10] To the same order, spin wave analysis of double-exchange magnets has been done in D. I. Golosov, Phys. Rev. Lett.

84, 3974 (2000); N. Shannon and A. V. Chubukov, Phys.

Rev. B **65**, 104418 (2002)).